

# Mechanical parameters detection in stepped shafts using the FEM based IET

Wenlei Song, Jiawei Xiang\* and Yongteng Zhong

College of Mechanical & Electrical Engineering, Wenzhou University, Wenzhou, 325035, P.R. China

(Received February 13, 2017, Revised July 15, 2017, Accepted July 19, 2017)

**Abstract.** This study suggests a simple, convenient and non-destructive method for investigation of the Young's modulus detection in stepped shafts which only utilizes the first-order resonant frequency in flexural mode and dimensions of structures. The method is based on the impulse excitation technique (IET) to pick up the fundamental resonant frequencies. The standard Young's modulus detection formulas for rectangular and circular cross-sections are well investigated in literatures. However, the Young's modulus of stepped shafts can not be directly detected using the formula for a beam with rectangular or circular cross-section. A response surface method (RSM) is introduced to design numerical simulation experiments to build up experimental formula to detect Young's modulus of stepped shafts. The numerical simulation performed by finite element method (FEM) to obtain enough simulation data for RSM analysis. After analysis and calculation, the relationship of flexural resonant frequencies, dimensions of stepped shafts and Young's modulus is obtained. Numerical simulations and experimental investigations show that the IET method can be used to investigate Young's modulus in stepped shafts, and the FEM simulation and RSM based IET formula proposed in this paper is applicable to calculate the Young's modulus in stepped shaft. The method can be further developed to detect mechanical parameters of more complicated structures using the combination of FEM simulation and RSM.

**Keywords:** nondestructive evaluation; impulse excitation technique; finite element simulation; response surface method; mechanical parameters detection

## 1. Introduction

Young's modulus is mechanical property of linear elastic solid material. Usually, it is the basic parameter for numerical simulations and damage detections. Therefore, it becomes essential to obtain the accurate value of Young's modulus for mechanical structures. The IET method is a non-destructive testing method covers determination of the dynamic elastic properties of elastic materials, which is based on the structures possess specific mechanical resonant frequencies that are determined by the elastic modulus, mass, and geometry (Alfano *et al.* 2007). The IET method is easy to perform and requires a very short time. In this technique, dynamic Young's modulus can be calculated directly using the data of resonant frequency and dimensions. It is helpful for mechanical engineer if the Young's modulus of structures can be calculated using an experimental formula. There are different strategies suggested for Young's modulus detection purposes depending on the type of the mode parameters used: natural frequency, displacement signal, loading force, deflection (Zeng *et al.* 2014, Zhang *et al.* 2013, Sousa *et al.* 2014). All of these have their advantages and disadvantages. The natural frequencies are commonly used to detect the

dynamic modulus of structures by comparison.

The IET method for the measurement of dynamic Young's modulus that is based on the resonant frequency of a structure present a very attractive possibility since the resonant frequency is quite easy and convenient to obtain from experiment. Yang *et al.* (2013, 2014a,b) developed wave motion analysis in arch structures via wavelet finite element method to detect damages. Zhang *et al.* (2015, 2016a,b) proposed several novel methods for vibration control using numerical model. Wang *et al.* (2011) presented Daubechies wavelet finite element method and genetic algorithm for detection of pipe crack. Xiang *et al.* (2012, 2013, 2014) developed identification of damage locations based on vibration analysis. Jiang *et al.* (2016) proposed an approach for rolling bearing fault diagnosis using numerical model. Soltanmalek *et al.* (2016) developed free vibration analysis of functionally graded fiber reinforced cylindrical panels by a three dimensional mesh-free model. Mei and Sha (2016) developed analytical and experimental study of vibrations in simple spatial structures. Zhang *et al.* (2015) presented a multi-resolution analysis for damage identification based finite element model updating method. Li *et al.* (2015) developed structural damage identification using numerical and experimental studies. Munoz-Abella (2012) developed a non-destructive method for elliptical cracks identification in shafts based on wave propagation signals and genetic algorithms. Yang *et al.* (2017a,b) presented an approach for damage detection in beams via modal curvature analysis. However, the mechanical parameters are basic parameters for numerical simulation and can not be theoretically

---

\*Corresponding author, Professor  
E-mail: wxw8627@163.com

obtained accurately. Therefore, the dynamic Young's modulus detection methods associated with frequency measurement have drawn special attention in the open accessible literature (Spinner *et al.* 1960, Kubojima *et al.* 2015, Pradhan *et al.* 2015). As the mechanical parameters of materials are often changed in production, it is very important to accurately know its property data. Generally, there are two procedures to accomplish the dynamic Young's modulus detection in structures. The first procedure is picking up the vibration signals of structures.

The second procedure is analyzing the vibration signals and getting the fundamental resonant frequency. When the resonant frequency is known and the dynamic Young's modulus can be calculated using the relationship of resonant frequencies and dynamic Young's modulus.

The impulse excitation technique (IET) is presented to measure the mechanical parameters of engineering materials using the standard uniform specimens including rectangular and circular cross-sections. The mechanical parameters detection formulas were well established for the standard uniform specimens with uniform rectangular and circular cross-section, which is described in an ASTM standard (ASTM E 2001). Recently, the technique has been used for the determination of mechanical parameters of different materials (ZnO ceramics, particulate composites, albite glass, ceramics, concrete and ceramic particle reinforced aluminum) in standard specimens (De Oliveira *et al.* 2012, Hauert *et al.* 2009, Bahr *et al.* 2013, Chiu *et al.* 1991, Lugovy *et al.* 2016, Popovics *et al.* 2000, Roebben *et al.* 2002, Schmidt *et al.* 2005, Tognana *et al.* 2010, Swarnakar *et al.* 2009, Zhang *et al.* 2013, Rupitsch *et al.* 2011). The technique has also been employed to determine mechanical parameters of materials in high temperature or room temperature (Pabst *et al.* 2016, Roebben *et al.* 1997, Bahr *et al.* 2013, Guillot *et al.* 2011, Behmanesh *et al.* 2016).

IET consists of exciting a test object by means of a light external mechanical impulse and of the analysis of the transient resonant vibration during the subsequent free decay, which may be done mechanically or acoustically. This excitation is given in such a way as to favor the desired vibration mode. The test is easy to perform and requires a very short time, a couple of seconds. The mechanical stresses that are applied to the specimen are minute. This also means that the test is virtually non-destructive. Dynamic Young's modulus can be calculated from the data of resonant frequency, mass, dimensions of the excited structure, and Poisson's ratio (ASTM 2001).

However, all of previous researchers did the analysis of mechanical parameters is about standard uniform specimens. In this work, the performance of the IET method for more complicated engineer structures is investigated, such as stepped shaft, etc. Further, if the existing mechanical parameters detection formulas can not provide the agreeable results, we proposed a hybrid approach using FEM simulation and RSM to obtain the experimental formula.

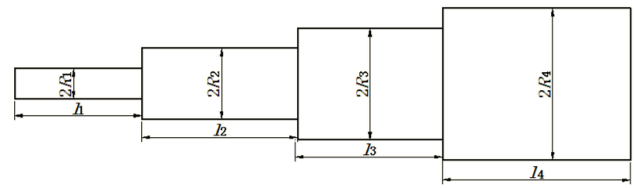


Fig. 1 Schematic diagram of the stepped shaft

## 2. The IET formula using numerical simulation and response surface method

### 2.1 Impulse excitation technique

The IET measures the fundamental resonant frequency of stepped shafts of suitable geometry by exciting them mechanically with an impulse tool. A transducer senses the resulting mechanical vibrations of stepped shafts and transforms them into electric signals. Support locations, impulse locations and signal pick-up points are selected to induce and measure specific modes of the transient vibrations. The signals are analyzed and the fundamental resonant frequency is isolated and measured by the signal analyzer, which provides a numerical reading that is first-order flexural resonant frequency of stepped shafts vibration. The appropriate fundamental resonant frequencies and dimensions of the stepped shafts are used to calculate dynamic Young's modulus.

### 2.2 Dynamic Young's modulus

For the fundamental flexural frequency of stepped shafts, there is no existing formula to use to calculate the Young's modulus because of the correction factor is difficult to determine accurately. The available and applicable formula can be presented through the finite element method (FEM) simulations and response surface method (RSM) based IET. Response surface method (RSM) designs a series of experimental combinations for numerical simulations, and numerical simulations based finite element method (FEM) provides enough simulation data for response surface method.

Response surface method (RSM) (Unal 2016) was used to systemically investigate the effect of a wide range of independent and dependent variables. A three-level box-behken design with five factors was selected to examine the unified objective. Experimental factors design can be seen in Table 1 and the schematic diagram of the stepped shaft is shown in Fig. 1.

A series of experimental combinations are designed based on the levels of these variables using design-expert software. The number of experimental combinations is 46 shown in Table 2.

The numerical simulations for every experimental case are performed using FEM software ANSYS. The diagram of stepped shafts and the displacement locations located in flexure node lines are shown in Fig. 2(a).

Table 1 Levels of process parameters used in response surface method

Code	Process parameters	Levels		
		0	1	2
$R_1$	The radius of first step of stepped shaft (m)	0.0165	0.0195	0.0225
$R_2$	The radius of second step of stepped shaft (m)	0.0230	0.0260	0.0290
$R_3$	The radius of third step of stepped shaft (m)	0.0295	0.0325	0.0355
$R_4$	The radius of fourth step of stepped shaft (m)	0.0360	0.0390	0.0420
$E$	The dynamic Young's modulus (GPa)	170	190	210

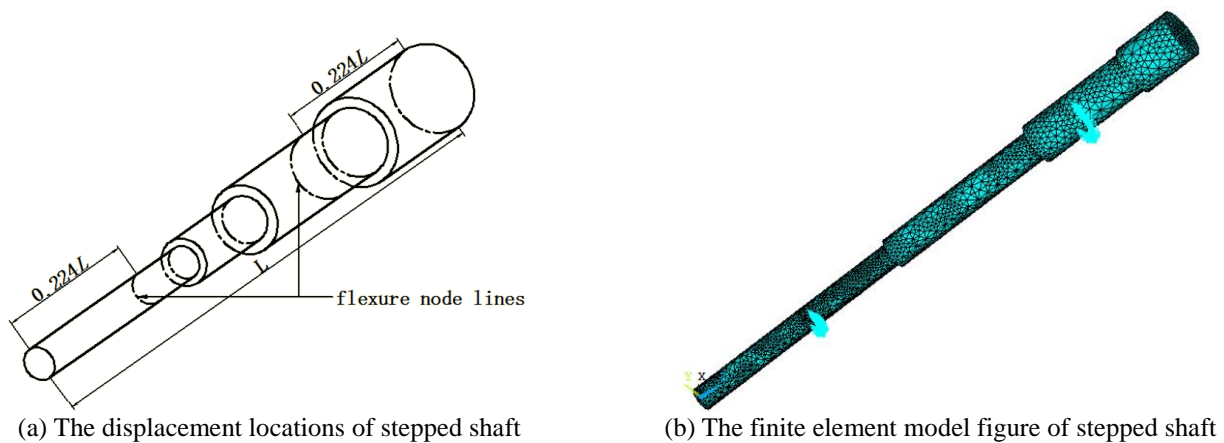


Fig. 2 Stepped shaft tested for flexural vibration

The finite element model figure of stepped shaft is shown in Fig. 2(b). Steel is chosen as the material of stepped shafts because steel is a common metal for mechanical engineers. "Solid 186" element was applied in ANSYS program to conduct simulation of stepped shafts in steel (set parameters as:  $\mu = 0.3$ ,  $\rho = 7860 \text{ kg/m}^3$ ). Modal analysis is performed to get the resonant frequency  $f$  in flexural modes. According to the computation, the first-order flexural resonant frequency  $f$  are obtained and recorded in Table 2.

Regression analysis is performed for each dependent variable using design-expert software. Response surface analysis was also applied to the data from box-behnken design for modeling and prediction of the relationship between Young's modulus  $E$  and other selected factors. The analysis of variance (ANOVA) for response surface reduced quadratic model is shown in Table 3.

The fitting was done using a second-order model for each response. The Model F-value of 701.3 implies the model is significant. There is only a 0.01% chance that a "Model F-Value" this large could occur due to noise. Values of "Prob > F" less than 0.0500 indicate model terms are significant.

In the present investigation,  $R_1, R_2, R_3, R_4, f, R_1R_2, R_1f, R_2R_4, R_2f, R_3R_4, R_3f, R_4f, R_1^2, R_2^2, R_3^2, R_4^2, f^2$  are significant model terms.

Table 4 shows the characteristic value of the model. The value of R-squared was 0.9976 shows that 99.76% of experimental data confirms the compatibility with the data predicted by the model. The "Pred R-squared" of 0.9962 is in reasonable agreement with the "Adj R-squared" of 0.9910. "Adeq Precision" measures the signal to noise ratio. A ratio greater than 4 is desirable. The ratio of 89.8213 indicates an adequate signal. This model can be used to navigate the design space.

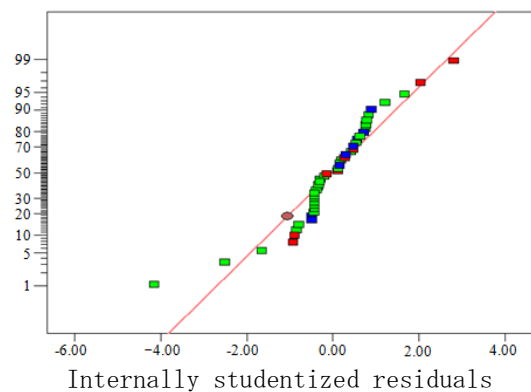


Fig. 3 Normal plot of residuals

Table 2 Experimental cases of response surface methodology

Case	$R_1$ (m)	$R_2$ (m)	$R_3$ (m)	$R_4$ (m)	$f$ (Hz)	$E$ (GPa)
1	0.0195	0.026	0.0355	0.042	181.194	190
2	0.0165	0.026	0.0295	0.039	164.753	190
3	0.0195	0.029	0.0295	0.039	195.784	190
4	0.0195	0.029	0.0325	0.042	193.346	190
5	0.0195	0.026	0.0325	0.039	185.404	190
6	0.0195	0.023	0.0355	0.039	166.373	190
7	0.0225	0.026	0.0355	0.039	197.843	190
8	0.0225	0.023	0.0325	0.039	172.070	190
9	0.0195	0.026	0.0295	0.039	193.365	210
10	0.0165	0.026	0.0325	0.039	174.013	210
11	0.0195	0.029	0.0355	0.039	198.261	190
12	0.0225	0.026	0.0295	0.039	194.852	190
13	0.0195	0.026	0.0325	0.039	185.404	190
14	0.0195	0.026	0.0325	0.039	185.404	190
15	0.0195	0.026	0.0355	0.039	175.809	190
16	0.0195	0.029	0.0325	0.036	201.517	190
17	0.0225	0.026	0.0325	0.039	207.160	210
18	0.0225	0.026	0.0325	0.036	202.729	190
19	0.0195	0.026	0.0325	0.042	189.736	210
20	0.0195	0.029	0.0325	0.039	186.892	170
21	0.0195	0.023	0.0325	0.042	160.893	190
22	0.0195	0.029	0.0325	0.039	207.719	210
23	0.0225	0.026	0.0325	0.042	191.173	190
24	0.0225	0.029	0.0325	0.039	215.881	190
25	0.0195	0.026	0.0325	0.042	170.712	170
26	0.0165	0.026	0.0325	0.039	156.566	170
27	0.0165	0.023	0.0325	0.039	154.131	190
28	0.0195	0.026	0.0295	0.039	173.977	170
29	0.0195	0.026	0.0295	0.036	189.094	190
30	0.0165	0.026	0.0355	0.039	165.621	190
31	0.0195	0.026	0.0325	0.039	185.404	190
32	0.0195	0.026	0.0325	0.036	199.913	210
33	0.0165	0.026	0.0325	0.042	161.761	190
34	0.0165	0.029	0.0325	0.039	170.737	190
35	0.0195	0.026	0.0295	0.042	178.491	190
36	0.0195	0.023	0.0325	0.039	174.840	210
37	0.0195	0.023	0.0295	0.039	165.334	190
38	0.0195	0.023	0.0325	0.036	171.654	190
39	0.0195	0.026	0.0355	0.039	195.401	210
40	0.0225	0.026	0.0325	0.039	186.389	170
41	0.0165	0.026	0.0325	0.036	169.078	190
42	0.0195	0.023	0.0325	0.039	157.309	170
43	0.0195	0.026	0.0325	0.039	185.404	190
44	0.0195	0.026	0.0355	0.036	190.765	190
45	0.0195	0.026	0.0325	0.036	179.869	170
46	0.0195	0.026	0.0325	0.039	185.404	190

Table 3 The analysis of variance table

Source	Sum of Squares ( $\times 10^{19}$ )	df	Mean Square ( $\times 10^{19}$ )	F Value	p-value Prob >F	The quality of model
Model	639	17	37.600	701.300	< 0.0001	significant
$R_1$	361	1	361	6737.393	< 0.0001	
$R_2$	362	1	362	6756.693	< 0.0001	
$R_3$	671	1	6.710	125.245	< 0.0001	
$R_4$	126	1	126	2359.822	< 0.0001	
$f$	551	1	551	10285.800	< 0.0001	
$R_1 R_2$	1.970	1	1.970	36.8618	< 0.0001	
$R_1 f$	0.477	1	0.477	8.898	0.0059	
$R_2 R_4$	2.750	1	2.750	51.437	< 0.0001	
$R_2 f$	0.686	1	0.686	12.815	0.0013	
$R_3 R_4$	0.273	1	0.273	5.099	0.0319	
$R_3 f$	0.491	1	0.491	9.163	0.0053	
$R_4 f$	1.110	1	1.110	20.662	< 0.0001	
$R_1^2$	11.900	1	11.900	222.082	< 0.0001	
$R_2^2$	10.100	1	10.100	187.666	< 0.0001	
$R_3^2$	0.949	1	0.949	17.714	0.0002	
$R_4^2$	0.234	1	0.234	4.371	0.0458	
$f^2$	0.081	1	0.081	1.506	0.2300	
Residual	1.500	28	0.054			
Lack of Fit	1.500	23	0.065			
Pure Error	0	5	0			
Cor Total	640	45				

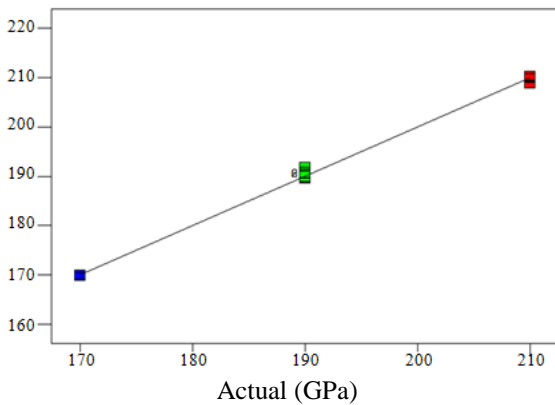


Fig. 4 Predicted vs. actual

Normal plot of residuals (as shown in Fig. 3) shows that the errors are distributed normally. Moreover, Fig. 4 also shows each experimental value matches well with its predicted value.

After conducting the experiments the obtained data were modeled and an experimental formula to predict  $E$  is obtained by

$$\begin{aligned}
 E = & 2.15196 \times 10^{11} - 2.15307 \times 10^{13} R_1 - 2.02443 \times 10^{13} \\
 & R_2 - 1.70041 \times 10^{12} R_3 + 6.24694 \times 10^{12} R_4 + 3835003975f \\
 & - 9.04594 \times 10^{14} R_1 R_2 - 67759500560 R_1 f - 4.07318 \times 10^{14} \\
 & R_2 R_4 - 82762415004 R_2 f - 9.40012 \times 10^{13} R_3 R_4 - 1520168 \\
 & 9270 R_3 f + 32685835169 R_4 f + 1.1947 \times 10^{15} R_1^2 + 1.11873 \times 10^{15} \\
 & R_2^2 + 1.15113 \times 10^{14} R_3^2 + 6.08567 \times 10^{13} R_4^2 + 2536349.853 f^2
 \end{aligned} \tag{1}$$

To prove the feasibility of the present method, numerical simulations are performed to detect dynamic Young's modulus of stepped shafts.

Suppose the stepped shaft dimensions are shown in Table 5 and the schematic diagram of the stepped shaft is shown in Fig. 1. The material properties of the stepped shaft are: Young's modulus  $E = 2.1 \times 10^{11} Pa$ , material density  $\rho = 7860 kg/m^3$ , and Poisson's ratio  $\mu = 0.3$ . The displacement is located in flexure node lines shown in Fig. 2.

The first-order flexural resonant frequency is recorded in Table 6.

Table 4 The Characteristic value of the model

Std. Dev.	$7.32 \times 10^8$	R-Squared	0.9976
Mean	$1.9 \times 10^{11}$	Adj R-Squared	0.9962
C.V. %	0.3851	Pred R-Squared	0.9910
PRESS	$5.74 \times 10^{19}$	Adeq Precision	89.8213

Table 5 The geometry dimensions of steel stepped shafts

Case	$R_1$ (m)	$R_2$ (m)	$R_3$ (m)	$R_4$ (m)	$l_1$ (m)	$l_2$ (m)	$l_3$ (m)	$l_4$ (m)
1	0.0195	0.026	0.0295	0.039				
2	0.0165	0.026	0.0325	0.039				
3	0.0225	0.026	0.0325	0.039	0.400	0.300	0.200	0.100
4	0.0195	0.023	0.0325	0.039				
5	0.0195	0.026	0.0355	0.039				

Table 6 The first-order flexural resonant frequency for stepped shafts

Case	1	2	3	4	5
$f$ (Hz)	193.365	174.013	207.16	174.84	195.401

Table 7 The calculation results of Young's modulus and absolute relative errors for stepped shafts

Case	1	2	3	4	5
$E^*$ (GPa)	210.5375	208.3833	210.0771	208.8293	209.8368
$\mathcal{E}$ (%)	0.2559	0.7698	0.0367	0.5574	0.0777

When the first-order flexural resonant frequency  $f$  for the stepped shaft is known, the Young's modulus  $E^*$  can be calculated using Eq. (1). Besides, the absolute relative errors of the dynamic Young's modulus  $\mathcal{E}$  between the measured and theoretical values can be calculated by

$$\mathcal{E} = \left| \frac{E^* - E}{E} \right| \times 100 \quad (2)$$

The calculation results of Young's modulus  $E^*$  and absolute relative errors  $\mathcal{E}$  for the stepped shafts are recorded in Table 7. For the five cases, the relative errors  $\mathcal{E}$  are varying from 0.0367% to 0.7698%.

The above numerical simulations clearly demonstrate that the mechanical parameters detection using IET for stepped shaft is efficient.

### 3. Experimental investigations

#### 3.1 Experimental setups

This IET method measures the fundamental resonant frequency of structures by exciting them mechanically with an impact hammer.

An overall description of the signal flow in the experiment is summarized as follows. First, the excitation impulse force exerted on the stepped shaft by an impact hammer. The accelerometer signal is acquired and sent to computer through the signal acquisition and analysis system (AVANT MI-7016) to perform fast Fourier transform (FFT) analysis, and the fundamental resonant frequency is isolated and measured. Considering the testing errors, five

replications are performed for per experiment. The average measured flexural resonant frequency  $f$  is used for calculation. The photographs of experimental structures and experimental setups are shown in Fig. 5. The stepped shaft hanged on flexure node lines by elastic wires.

Table 8 shows the geometry dimensions of experimental steel stepped shaft.



(a) Experimental structure



(b) Experimental test setup

Fig. 5 Photographs of the structure and experimental test setup for stepped shaft in flexural mode

Table 8 The geometry dimensions of steel stepped shaft in experiments

Case	$R_1$ (m)	$R_2$ (m)	$R_3$ (m)	$R_4$ (m)	$l_1$ (m)	$l_2$ (m)	$l_3$ (m)	$l_4$ (m)
1	0.020	0.027	0.033	0.039	0.400	0.300	0.200	0.100
2	0.017	0.024	0.030	0.037				

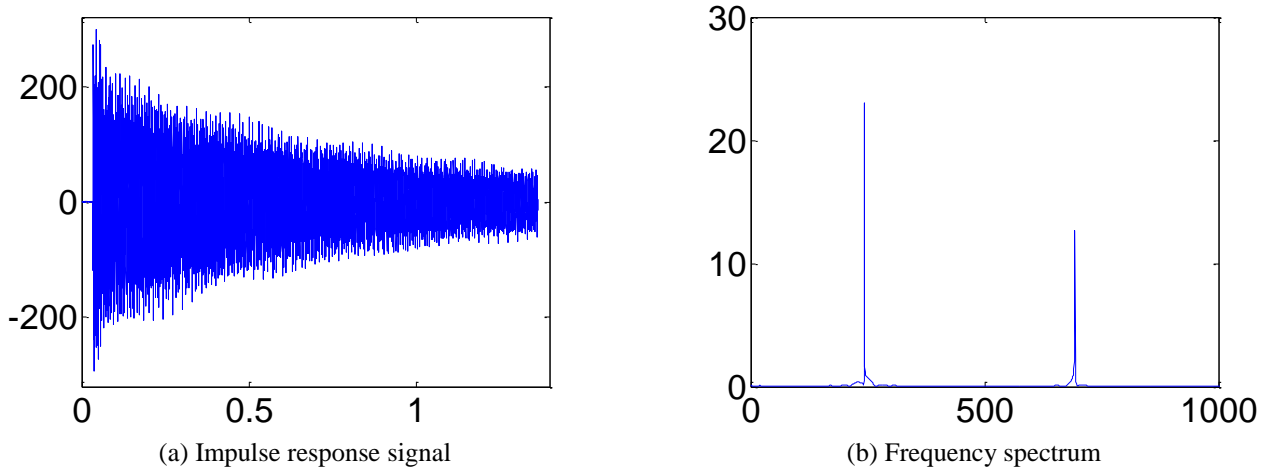


Fig. 6 The measured impulse response signal and the corresponding frequency spectrum of stepped shafts for Case 1

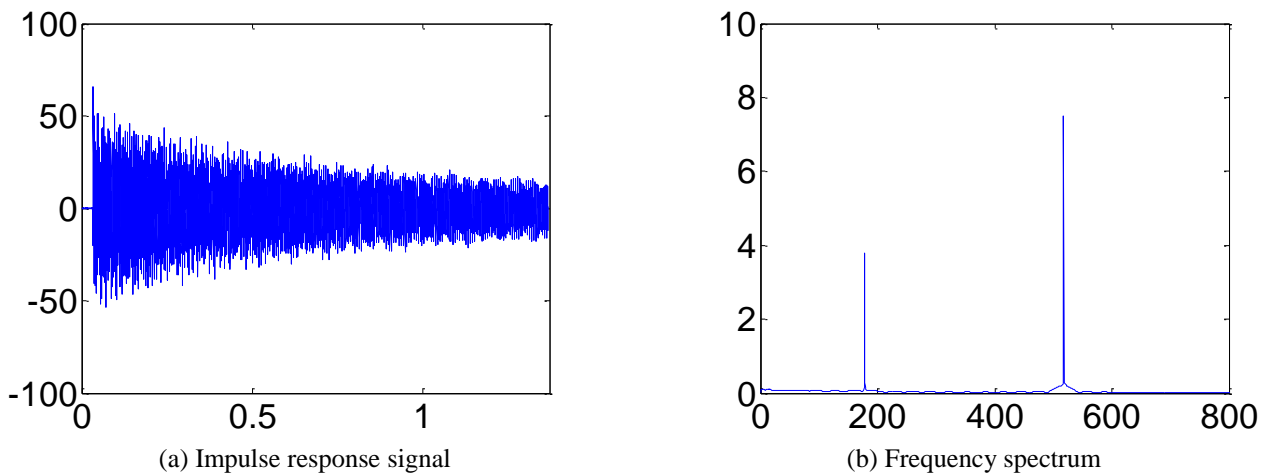


Fig. 7 The measured impulse response signal and the corresponding frequency spectrum of stepped shafts for Case 2

### 3.2 Fundamental flexural resonant frequency measurement

Strike the stepped shaft lightly, either at the center of them or at the opposite end of them from the detecting accelerometer. Use the average of these five readings to determine the fundamental flexural resonant frequency of each case.

The measured impulse response signal and the corresponding frequency spectrum of steel stepped shafts in flexural mode are shown in Figs. 6 and 7.

Table 9 The results of experiments

Case	1	2
$f$ (Hz)	201.78	168.5
$E$ (GPa)	207.80	202.24
$\mathcal{E}$ (%)	0.87	1.82

The measured first-order flexural resonant frequencies  $f$  for the stepped shafts are shown in Table 9.

Similar to the numerical simulation in Section 2, when the first-order resonant frequency  $f$  for stepped shafts is measured, Young's modulus  $E^*$  will be calculated using Eq. (1). Table 9 also gives the absolute relative errors of the mechanical parameters  $\varepsilon$  between the measured and theoretical values can be calculated using Eq. (2).

As shown in Table 9, the relative errors  $\mathcal{E}$  for the stepped shafts are varying from 0.87% to 1.82%.

The above experiment investigations clearly demonstrate that the Young's modulus detection using the standard IET, the FEM simulation and RSM based IET can be applied to more complicate structures, such as stepped shafts.

#### 4. Conclusions

This paper suggests a simple procedure for dynamic Young's modulus detection for stepped shaft which is based on the impulse excitation technique (IET). In our investigation, the Young's modulus of stepped shaft can not be directly detected using the formula for a beam with rectangular or circular cross-section. Therefore, a hybrid method using FEM simulation and RSM is introduced to design numerical simulation experiments to build up experimental formula to detect Young's modulus of stepped shafts.

The procedure involves two steps. The first step is the acquisition of vibration signal in flexural mode for structures. The second procedure is analyzing the vibration signals and getting the first-order flexural resonant frequency. Then the values of frequencies are submitted into the IET formula to calculate the dynamic Young's modulus of stepped shafts. In the present method, simulations and experimental investigations are applied to prove the accuracy of formulas. The numerical and experimental results show that the IET is applicable for Young's modulus detection for stepped shafts.

The hybrid method using FEM simulation and RSM may be helpful to develop agreeable experimental formulas to detect mechanical parameters for complicated structures.

#### Acknowledgments

The authors are grateful to the support from the National Science Foundation of China (Nos. 51575400, 51505339), the Zhejiang Provincial Natural Science Foundation of China (Nos. LR13E050002, LQ161050005), the Wenzhou Technologies R&D Program of China (No. G20140047).

#### References

Alfano, M. and Pagnotta, L. (2007), "A non-destructive technique for the elastic characterization of thin isotropic plates", *Ndt. & E. Int.*, **40**(2), 112-120.

- ASTM, E. (2001), "Standard test method for dynamic Young's modulus, shear modulus, and Poisson's ratio by sonic resonance", *Annual Book of ASTM Standards 2001*.
- Bahr, O., Schaumann, P., Bollen, B. and Bracke, J. (2013), "Young's modulus and Poisson's ratio of concrete at high temperatures: Experimental investigations", *Mater. Design*, **45**, 421-429.
- Behmanesh, I. and Moaveni, B. (2016), "Accounting for environmental variability, modeling errors, and parameter estimation uncertainties in structural identification", *J. Sound. Vib.*, **374**, 92-110.
- Chiu, C.C. and Case, E.D. (1991), "Elastic modulus determination of coating layers as applied to layered ceramic composites", *Mat. Sci. Eng. A - Struct.*, **132**, 39-47.
- De Oliveira, A.P.N., Vilches, E.S., Soler, V.C. and Villegas, F.A.G. (2012), "Relationship between Young's modulus and temperature in porcelain tiles", *J. Eur. Ceram. Soc.*, **32**(11), 2853-2858.
- Guillot, F.M. and Trivett, D.H. (2011), "Complete elastic characterization of viscoelastic materials by dynamic measurements of the complex bulk and Young's moduli as a function of temperature and hydrostatic pressure", *J. Sound. Vib.*, **330**, 3334-3351.
- Hauert, A., Rossoll, A. and Mortensen, A. (2009), "Young's modulus of ceramic particle reinforced aluminium: Measurement by the Impulse Excitation Technique and confrontation with analytical models", *Compos. Part. A-Appl. S.*, **40**(4), 524-529.
- Jiang, B.Z., Xiang, J.W. and Wang, Y.X. (2016), "Rolling bearing fault diagnosis approach using probabilistic principal component analysis denoising and cyclic bispectrum", *J. Vib. Control*, **22**(10), 2420-2433.
- Kubojima, Y., Kato, H., Tonosaki, M. and Sonoda, S. (2015), "Measuring young's modulus of a wooden bar using flexural vibration without measuring its weight", *Bio Resources*, **11**(1), 800-810.
- Li, J., Hao, H., and Lo, J.V. (2015), "Structural damage identification with power spectral density transmissibility: numerical and experimental studies", *Smart Struct. Syst.*, **15**(1), 15-40.
- Liu, J.X., Zhang, X.W. and Chen, X.F. (2016a), "Modeling and active vibration control of a coupling system of structure and actuators", *J. Vib. Control*, **22**(2), 382-395.
- Lugovy, M., Slyunyayev, V., Orlovskaya, N., Mitrentsis, E., Aneziris, C.G., Graule, T. and Kuebler, J. (2016), "Temperature dependence of elastic properties of ZrB 2-SiC composites", *Ceram. Int.*, **42**(2), 2439-2445.
- Mei, C. and Sha, H. (2016), "Analytical and experimental study of vibrations in simple spatial structures", *J. Vib. Control*, **22**(17), 3711-3735.
- Munoz-Abella, B., Rubio, L. and Rubio, P. (2012), "A non-destructive method for elliptical cracks identification in shafts based on wave propagation signals and genetic algorithms", *Smart Struct. Syst.*, **10**(1), 47-65.
- Pabst, W., Gregorová, E., Kloužek, J., Kloužková, A., Zemenová, P., Kohoutková, M. and Všianský, D. (2016), "High-temperature Young's moduli and dilatation behavior of silica refractories", *J. Eur. Ceram. Soc.*, **36**(1), 209-220.
- Popovics, J.S., Kolluru, S.V. and Shah, S.P. (2000), "Determining elastic properties of concrete using vibrational resonance frequencies of standard test cylinders", *Cement, Concrete Aggr.*, **22**(2), 81-89.
- Pradhan, R., Dhara, A.K., Panchadhyayee, P. and Syam, D. (2015), "Determination of Young's modulus by studying the flexural vibrations of a bar: experimental and theoretical approaches", *Eur. J. Phys.*, **37**(1), 015001.
- Roebben, G. and Omer, V.D.B. (2002), "Recent advances in the

- use of the impulse excitation technique for the characterisation of stiffness and damping of ceramics, ceramic coatings and ceramic laminates at elevated temperature”, *Key Eng. Mater.*, **206**, 621-624.
- Roebben, G., Bollen, B., Brebels, A., Van Humbeeck, J. and Van der Biest, O. (1997), “Impulse excitation apparatus to measure resonant frequencies, elastic moduli, and internal friction at room and high temperature” *Rev. Sci. Instrum.*, **68**(12), 4511-4515.
- Rupitsch, S.J., Ilg, J., Sutor, A., Lerch, R. and Döllinger, M. (2011), “Simulation based estimation of dynamic mechanical properties for viscoelastic materials used for vocal fold models”, *J. Sound. Vib.*, **330**(18), 4447-4459.
- Schmidt, R., Wicher, V. and Tilgner, R. (2005), “Young's modulus of moulding compounds measured with a resonance method”, *Polym. Test.*, **24**(2), 197-203.
- Soltanmaleki, A., Foroutan, M. and Alihemmati, J., (2016), “Free vibration analysis of functionally graded fiber reinforced cylindrical panels by a three dimensional mesh-free model”, *J. Vib. Control*, **22**(19), 4087-4098.
- Sousa, F.J., Dal Bó, M., Guglielmi, P.O., Janssen, R. and Hotza, D. (2014), “Characterization of Young's modulus and fracture toughness of albite glass by different techniques”, *Ceram. Int.*, **40**(7), 10893-10899.
- Spinner, S., Reichard, T.W. and Tefft, W.E., (1960), “A comparison of experimental and theoretical relations between young's modulus and the flexural and longitudinal resonance frequencies of uniform bars”, *J. Res. Natl. Bur. Stand. Phys. Chem.*, **64**(2), 147-155.
- Swarnakar, A.K., Donzel, L., Vleugels, J. and Biest, O.V.D. (2009), “High temperature properties of ZnO ceramics studied by the impulse excitation technique”, *J. Eur. Ceram. Soc.*, **29**(14), 2991-2998.
- Tognana, S., Salgueiro, W., Somoza, A. and Marzocca, A. (2010), “Measurement of the Young's modulus in particulate epoxy composites using the impulse excitation technique”, *Mat. Sci. Eng. A-Struct.*, **527**(18), 4619-4623.
- Unal, O. (2016), “Optimization of shot peening parameters by response surface methodology”, *Surf. Coat. Tech.*, **305**, 99-109.
- Wang, Y.M., Chen, X.F. and He, Z.J. (2011), “Daubechies wavelet finite element method and genetic algorithm for detection of pipe crack”, *Nondestruct. Test. Eva.*, **26**(1), 87-99.
- Xiang, J.W., Matsumoto, T. and Long, J.Q. (2013), “Identification of damage locations based on operating deflection shape”, *Nondestruct. Test. Eva.*, **28**(2), 166-180
- Xiang, J.W., Matsumoto, T., Long, J.Q., Wang, Y.X. and Jiang, Z.S. (2012), “A simple method to detect cracks in beam-like structures”, *Smart Struct. Syst.*, **9**(4), 335-353.
- Xiang, J.W., Nackenhorst, U., Wang, Y.X., Jiang, Y.Y., Gao, H.F. and He, Y.M. (2014), “A new method to detect cracks in plate-like structures with through-thickness cracks”, *Smart Struct. Syst.*, **14**(3), 397-418.
- Yang, Z.B., Chen, X.F. and Jiang, Y.Y. (2014a), “Generalised local entropy analysis for crack detection in beam-like structures”, *Nondestruct. Test. Eva.*, **29**(2), 133-153.
- Yang, Z.B., Chen, X.F., Li, X., Jiang, Y.Y., Miao, H.H. and He, Z.J. (2014b), “Wave motion analysis in arch structures via wavelet finite element method”, *J. Sound. Vib.*, **333**(2), 446-469.
- Yang, Z.B., Chen, X.F., Yu, J., Liu, R., Liu, Z.H. and He, Z.J. (2013), “A damage identification approach for plate structures based on frequency measurements”, *Nondestruct. Test. Eva.*, **28**(4), 321-341.
- Yang, Z.B., Radzienski, M., Kudela, P. and Ostachowicz, W. (2017a), “Fourier spectral-based modal curvature analysis and its application to damage detection in beams”, *Mech. Syst. Signal. Pr.*, **84**, 763-781.
- Yang, Z.B., Radzienski, M., Kudela, P., and Ostachowicz, W. (2017b), “Damage detection in beam-like composite structures via Chebyshev pseudo spectral modal curvature”, *Compos. Struct.*, **168**, 1-12.
- Zeng, X., Wen, S., Li, M. and Xie, G. (2014), “Estimating Young's modulus of materials by a new three-point bending method”, *Adv. Mater. Sci. Eng.*, **2014**(1), 1-9.
- Zhang, E., Chazot, J.D., Antoni, J. and Hamdi, M. (2013), “Bayesian characterization of Young's modulus of viscoelastic materials in laminated structures”, *J. Sound. Vib.*, **332**(16), 3654-3666.
- Zhang, X., Gao, D.Y., Liu, Y. and Du, X. (2015), “A multi-resolution analysis based finite element model updating method for damage identification”, *Smart Struct. Syst.*, **16**(1), 47-65.
- Zhang, X.W., Chen, X.F., You, S.Q. and He, Z. (2015), “Active control of dynamic frequency responses for shell structures”, *J. Vib. Control*, **21**(14), 2813-2824.
- Zhang, X.W., Gao, R.X., Yan, R.Q., Chen, X.F., Sun, C. and Yang, Z.B. (2016b), “Multivariable wavelet finite element-based vibration model for quantitative crack identification by using particle swarm optimization”, *J. Sound. Vib.*, **375**, 200-216.

CC